CHIN. PHYS. LETT. Vol. 34, No. 7 (2017) 078503

Optical Field Confinement Enhanced Single ZnO Microrod UV Photodetector *

Ming Wei(魏铭), Chun-Xiang Xu(徐春祥)**, Fei-Fei Qin(秦飞飞), Arumugam Gowri Manohari, Jun-Feng Lu(卢俊峰), Qiu-Xiang Zhu(祝秋香)

State Key Laboratory of Bioelectronics, School of Biological Science and Medical Engineering, Southeast University, Nanjing 210096

(Received 27 March 2017)

ZnO microrods are synthesized using the vapor phase transport method, and the magnetron sputtering is used to decorate the Al nanoparticles (NPs) on a single ZnO microrod. The micro-PL and I–V responses are measured before and after the decoration of Al NPs. The FDTD stimulation is also carried out to demonstrate the optical field distribution around the decoration of Al NPs on the surface of a ZnO microrod. Due to an implementation of Al NPs, the ZnO microrod exhibits an improved photoresponse behavior. In addition, Al NPs induced localized surface plasmons (LSPs) as well as improved optical field confinement can be ascribed to an enhancement of ultraviolet (UV) response. This research provides a method for improving the responsivity of photodetectors.

PACS: 85.60.Bt, 85.60.Gz, 78.67.−n DOI: 10.1088/0256-307X/34/7/078503

As a direct band-gap semiconductor material with 3.37 eV and large exciton binding energy of 60 meV at room temperature, ZnO has been considered for a long time to be one of the ideal materials for ultraviolet photoluminescence, lasing and sensing applications. Over the past few decades, various kinds of ZnO materials including single crystal, thin film and micro/nano structures have been used in UV photoluminescence and sensing.[1−6] Compared with bulk materials, one-dimensional ZnO materials like microrods and nanowires are more suitable for the fabrication of a photodetector with high sensitivity and fast response due to their high surface-to-volume ratio. In 2002, Kind *et al.* reported a UV photodetector using a single ZnO nanowire.[7] Since then, great efforts have been made to one-dimensional ZnO photodetectors.[8,9] In 2013, Dai *et al.* also presented a UV photodetector with single ZnO microrods and introduced an optical whispering gallery mode effect to enhance the photocurrent and photoresponsivity.[10] However, the performance of devices based on raw ZnO materials are limited because of lattice defects and surface absorption, etc.[11−13]

Owing to the existence of coherent delocalized electron oscillations at an interface between metal and semiconductor, surface plasmons can greatly enhance the coupling efficiency of incident photons and electrons in the nearest metal-dielectric interface thus improving the optoelectronic performances of semiconductor devices. Liu *et al.* have obtained an enhanced electroluminescence behavior of ZnO nanorod array as Light emitting diodes (LEDs) with decorated Ag nanoparticles.[14] Moreover, Pei *et al.* reported a highly responsive UV photodetector of ZnO using the decoration of Pt NPs,[15] and Fan *et al.* also used the Au NPs as surface plasmons to fabricate the UV photodetector from ZnO.[16] Compared with traditional plasmonic materials such as Au, Ag and Pt, researchers considered Al as one of the promising candidates for the performance in blue and UV ranges due to its lower Fermi energy level and absorption peak appearing in the range of UV.[17]

In this Letter, a photodetector is fabricated with a single ZnO microrod based on the structure of metal-semiconductor-metal (MSM) and the plasmonic materials of Al NPs are decorated on the surface of the ZnO microrod. An improved UV response as well as excellent reproducibility is observed in the Al NPs decorated ZnO in comparison with that of a bare one. The micro-PL studies and FDTD simulation are carried out to reveal the inner mechanism. The optical whispering gallery mode effect and surface plasmons induced optical field confinement are attributed for the superior performance of the photodetector.

The ZnO microrods were synthesized using the vapor phase transport method.[18] In a typical process, the ZnO and graphite powders were mixed together as the source material with mass ratio of 1:1. Then, 0.85 g of the above mixed powders were placed in a quartz boat covered by a cleaned silicon substrate. After that, the boat was sent into a quartz tube and the temperature was fixed at 1050℃. The ZnO microrods can be formed on the silicon substrate after the reaction about 30 min. An individual ZnO microrod was picked up and placed flat on the SiO_2 substrate. Two In granules were tied on each end of the ZnO microrod as electrodes and the spacing of two electrodes was fixed as 5 mm. Then, the device was heated up to 60℃ for 30 min to attain a stable connection between the microrod and electrodes. In addition, Al NPs were decorated on the surface of the microrod by using magnetron sputtering in which the chamber

*Supported by the National Natural Science Foundation of China under Grant Nos 61475035 and 61275054, the Science and Technology Support Program of Jiangsu Province under Grant No BE2016177, and the Collaborative Innovation Center of Suzhou Nano Science and Technology.

**Corresponding author. Email: xcxseu@seu.edu.cn

© 2017 Chinese Physical Society and IOP Publishing Ltd

pressure was set as 2.0 Pa, the Ar flow was 50 sccm, the sputtering power was 100 W and the reaction time was 100 s.

The structure of the ZnO microrod was analyzed by using x-ray diffraction (XRD-7000, Shimadzu) with Cu Kα radiation and the morphology was characterized by a field emission scanning electron microscope (FESEM, Carl Zeiss Ultra Plus) equipped with an x-ray energy dispersive spectroscope (EDS, Oxford X-Max 50). The optoelectronic performances were measured using a semiconductor parameter system (Keithley 4200) and the device was excited by a 325 nm He-Cd laser at 100 mW/cm^2 (Kimmon IK3501R-G). The lasing spectra were recorded by a homemade micro-PL system with a spectrometer (SP2500i, Princeton) and an excitation source of 150 fs laser with a repetition rate of 1 kHz at 325 nm (OperA Solo, Coherent).

Figure 1(a) shows the SEM images of Al NPs decorated ZnO with cross sections. The diameter of the microrod is 11.96 μm whereas the radius of Al NPs is identified as 80 nm approximately. The elemental mapping profile is used to confirm the presence of all the elements including Zn, O and Al as shown. From the figure, it can also be noticed that the stoichiometric distribution of Zn and O elements is on the entire microrod while Al is uniformly distributed on the surface of the ZnO microrod. An existence of O element beyond the profile of the ZnO microrod is probably caused by the SiO_2 substrate. Furthermore, Fig. 1(b) represents the XRD pattern for bare ZnO microrods grown on the silicon substrate. All the diffraction peak position values are corresponding to ZnO with the wurtzite structure.

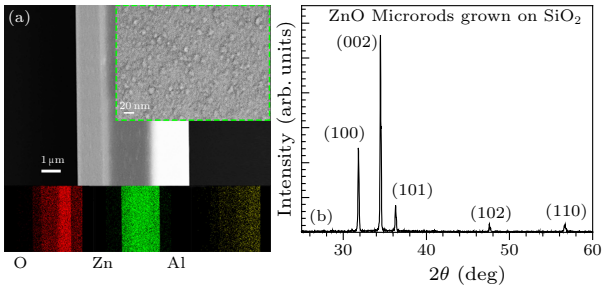

Fig. 1. (a) SEM image of a ZnO microrod with typical hexagonal cross section and O, Zn, Al element mapping images for an Al NPs decorated ZnO microrod. The insect shows the SEM image of Al NPs on a ZnO microrod. (b) X-ray diffraction of ZnO microrod grown on a silicon substrate.

Figure 2(a) demonstrates the I–V response of the device with a bare ZnO microrod under dark conditions and UV illumination. The current is increased linearly with respect to the applied voltage in the dark, which indicates the Ohmic contact between the microrod and electrodes. Figure 2(b) shows the I–V response of the device after the decoration of Al NPs. From the figure, it can be observed that the dark current is slightly increased while the UV illuminated photocurrent is achieved with an increase, which is 10 times greater than that of bare ZnO. Due to the Ohmic contact and the low work function of Al (4.3 eV), the free electrons can be transferred easily from Al NPs to the conduction band of ZnO thus resulting in the increase of the dark current.[19] Meanwhile, Al NPs induced surface plasmons couples with the ZnO microrod, resulting in increased energy absorption, thus the electron-hole generation process is accelerated and photocurrent enhanced.

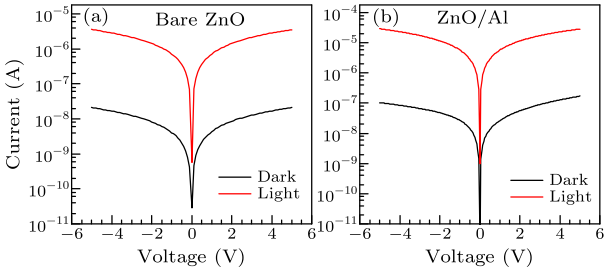

Fig. 2. The I–V curves for a photodetector based on (a) bare and (b) Al NPs decorated ZnO microrod in the dark and UV illumination.

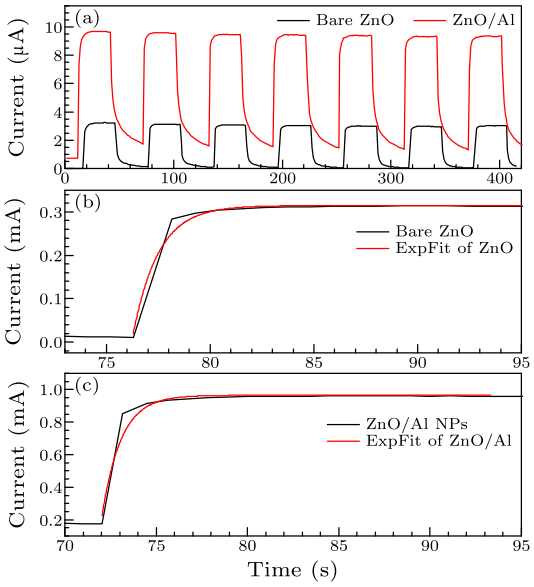

Fig. 3. (a) On/off switching of the device at 325 nm of UV illumination with 60 s cycle and bias voltage of 2.0 V. [(b), (c)] Enlarged portion for photocurrent rising process under UV illumination.

To further investigate the optoelectronic performances of the device, few cycles of photocurrent have been measured based on on/off switching as depicted in Fig. 3(a). In addition, each cycle has been controlled by an electrical shutter and both the turn-on and turn-off time are fixed as 30 s. The device exhibits a dramatic enhancement in light-to-dark current ratio after the decoration of Al NPs, and a steady state reproducibility during the cycles is obtained. Figures 3(b) and 3(c) present the enlarged photocurrent rising process under UV illumination and the rising times

are fitted using the exponential function[20]

$$I = I_0(1 - e^{-t/\tau_r}), \tag{1}$$

where I_0 is referred as the steady state photocurrent, and τ_r is denoted as the time constant for rising photocurrent. The estimated rising times of bare ZnO and an Al NPs decorated ZnO microrod are 1.22 s and 0.36 s, respectively. According to Eq. (1) the Al NPs decorated ZnO possesses a faster response rate. This may be caused due to an effect of surface plasmons of Al NPs.

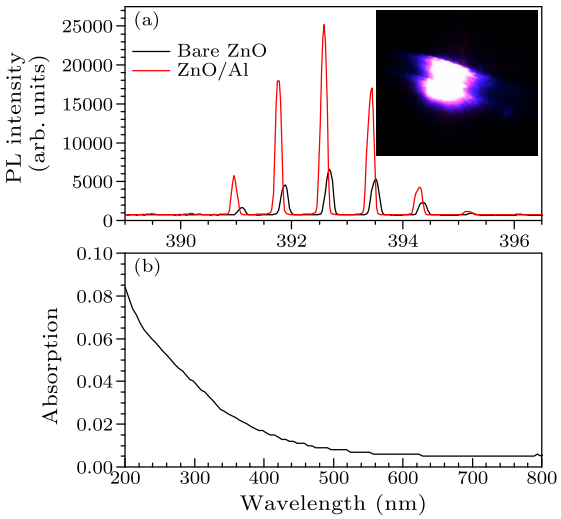

Fig. 4. (a) PL spectra for ZnO microrod before and after the decoration of Al NPs with the same excitation power. The inset shows an optical microscope image of single ZnO microrod. (b) UV-vis absorption spectrum of Al NPs.

A unique hexagonal prism interface of ZnO microrods generally provides an ideal WGM resonant cavity in the fabrication of UV laser devices, which is a well-known phenomenon.[21] The structure could effectively confine the light inside the cavity thus improving an interaction between light and matter which is also beneficial for photodetection. Here Al NPs have been implemented to further enhance an optical field confinement effect of a ZnO WGM cavity. Moreover, to illustrate the optical field confinement effect of the structure, micro-PL has been measured before and after the decoration of Al NPs. From Fig. 4(a), it can be noted that the microrod is presented in a clear WGM lasing mode because of its hexagonal structure. The emission peaks are identified at 391.13 nm, 391.87 nm, 392.67 nm, 393.51 nm, 394.35 nm and 395.22 nm. According to the WGM resonance equation,[22] the mode numbers of the resonance peaks situate in the range of 184–189. On the other hand, Fig. 4(b) illustrates an absorption spectrum of Al NPs on quartz substrates and the absorption edge is located around the UV range. Hence, the lasing intensity is enhanced in the Al NPs decorated ZnO microrod, which is five times greater than that of the bare one and the Q factor of the highest peak improves from 2825 to 3303. The result can be proposed that an enhancement of intensity may be spawned due to the absorption of Al NPs, thus the corresponding light energy can be transferred from Al NPs to the excitons of ZnO via resonant coupling with LSP modes.[23] In addition, the blueshift of the peaks predicts a better coupling efficiency between LSPs and excitons in a shorter wavelength range.

Figures 5(a) and 5(b) demonstrate the responsivity of a bare ZnO microrod UV photodetector before and after the decoration of Al NPs under illuminations at different wavelengths. The bias is fixed at 5.0 V. The spectra show the sensitivity of the device to UV light, and an improvement in responsivity in the UV region after the decoration of Al NPs. The results further convince the transfer process from Al NPs to ZnO via resonant coupling with LSP modes.

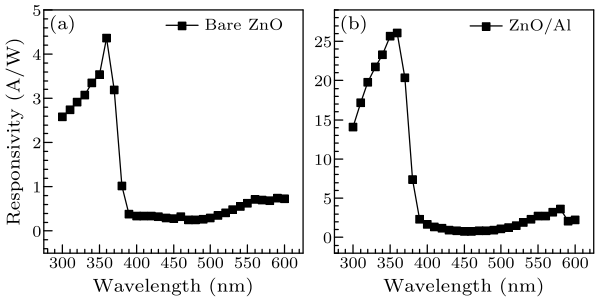

Fig. 5. Responsivity spectra of the ZnO microrod UV detector (a) without and (b) with Al NPs using different exciting wavelengths.

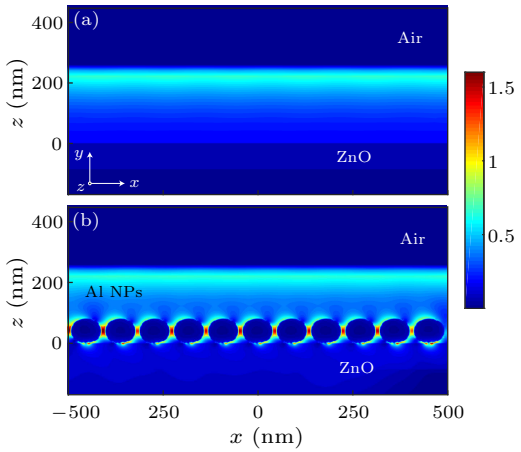

Fig. 6. FDTD simulated electric field distribution at an interface between bare ZnO and ZnO/Al NPs.

To further explore an optical confinement induced by surface plasmons of Al NPs, an electric field distribution on the interface between Al and ZnO has been calculated by finite-difference time-domain simulation. During the simulation, the Al NPs with a diameter of 80 nm consistent with the experiments are put on the surface of ZnO. Since the diameter of ZnO (11.96 μm) is much larger than that of Al NPs, the model is simplified and we set the ZnO surface as plane. The light source in the range of 200–700 nm is illuminated on the upper side of the sample along the y axis with an angle of 60° and the period bound-

ary condition is used in x and z directions whereas the perfect matched layer is used in the y direction. The electric field monitor is used to record the electric field distribution in the y–z plane and the results are depicted in Fig. 6. Because of LSP coupling, the light can be confined in an interface between Al and ZnO, which leads to the increase of the electric field intensity. This phenomenon is responsible for an enhancement of optical and electrical properties of the hybrid structure. Importantly, the resonant wavelength of Al is located near the absorption of the edge of ZnO according to Fig. 4(b), which possesses the resonant energy transfer thus resulting in improved performance of photoluminescence.[24]

LSP coupling is highly sensitive to the size and density distribution of nanoparticles. As shown in Fig. 1, the distribution of Al NPs is not perfectly uniform, which will result in a shift in the absorption peak. Thus the absorption spectrum in Fig. 4(b) demonstrates an absorption band instead of a sharp peak. To reveal the influence of particle size and distribution on LSP coupling, the electronic field distributions for different sizes and distributions are calculated. The peak electronic field intensity is shown in Fig. 7. As can be seen, the electronic field increases about 3–10 times when decorated with Al NPs, a higher electronic field enhancement factor appears for the particle size ranging in 50–100 nm and particle gap ranging in 0–10 nm. These ranges agree well with the SEM result of Fig. 1. On the other hand, the magnified electromagnetic field caused by LSP can increase the quantum efficiency. These are the reasons for superior optoelectronic performance of the photodetector as well.

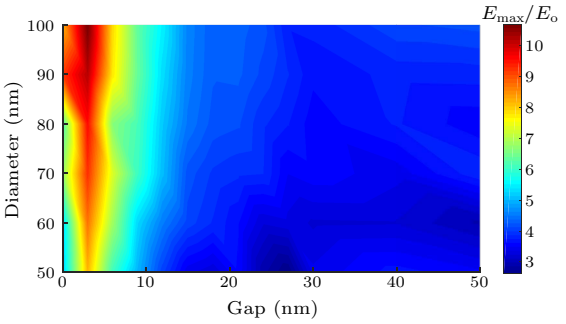

Fig. 7. Maximum electric field distribution on the surface of Al decorated ZnO with different diameters and particle distributions (with the monitor wavelength of 390 nm).

In summary, Al NPs decorated single ZnO microrod based MSM UV photodetector have been fabricated. Under UV illumination at 325 nm with an excitation source of the He-Cd laser, an enhanced photoresponsivity and light-to-dark ratio with 4-hold are observed. The micro-PL and FDTD simulation demonstrate the WGM effect and plasmons induced light confinement, attributed to superior performance of the device. The surface plasmons of Al NPs interact with excitons of ZnO microrods through direct resonant energy coupling which accelerates the decay of excitons thus results in enhanced photoresponsivity. Another reason for an enhancement of the device is owing to the hexagonal structure of ZnO microrods, which provides an ideal WGM cavity for the coupling process. These results provide an effective way for fabricating the UV photodetector with better photoresponse performance.

References

[1] Peng L, Hu L and Fang X 2013 *Adv. Mater.* **25** 5321
[2] Hassan J J, Mahdi M A, Kasim S J, Ahmed N M, Abu Hassan H and Hassan Z 2012 *Appl. Phys. Lett.* **101** 261108
[3] Wang X, Liao M Y, Zhong Y T, Zheng J Y, Tian W, Zhai T Y, Zhi C Y, Ma Y, Yao J N, Yoshio B and Golberg D 2012 *Adv. Mater.* **24** 3421
[4] Cheng G, Wu X, Liu B, Li B, Zhang X and Du Z 2011 *Appl. Phys. Lett.* **99** 203105
[5] Li J J, Gao Z Y, Xue X W, Li H M, Deng J, Cui B F and Zou D S 2016 *Acta Phys. Sin.* **65** 118104 (in Chinese)
[6] Qi X M, Peng W B, Zhao X L and He Y N 2015 *Acta Phys. Sin.* **64** 0198501 (in Chinese)
[7] Kind H, Yan H, Messer B, Law M and Yang P 2002 *Adv. Mater.* **14** 158
[8] Tsai D S, Lin C A, Lien W C, Chang H C, Wang Y L and He J H 2011 *ACS Nano* **5** 7748
[9] Xu Q, Cheng Q, Zhong J, Cai W, Zhang Z, Wu Z and Zhang F 2014 *Nanotechnology* **25** 055501
[10] Dai J, Xu C X, Xu X, Guo J, Li J T, Zhu G Y and Lin Y 2013 *ACS Appl. Mater. Interfaces* **5** 9344
[11] Seo H, Park C J, Cho Y J, Kim Y B and Choi D K 2010 *Appl. Phys. Lett.* **96** 232101
[12] Law J B K and Thong J T L 2006 *Appl. Phys. Lett.* **88** 133114
[13] Ahn S E, Lee J S, Kim H, Kim S, Kang B H, Kim K H and Kim G T 2004 *Appl. Phys. Lett.* **84** 5022
[14] Liu W Z, Xu H Y, Wang C L, Zhang L X, Zhang C, Sun S Y and Liu Y C 2013 *Nanoscale* **5** 8634
[15] Pei J, Jiang D, Zhao M, Duan Q, Liu R and Sun L 2016 *Appl. Surf. Sci.* **389** 1056
[16] Fan H, Sun M, Ma P, Yin M, Lu L, Xue X and Zhu X 2016 *Nanotechnology* **27** 365303
[17] West P R, Ishii S, Naik G V, Emani N K, Shalaev V M and Boltasseva A 2010 *Laser Photon. Rev.* **4** 795
[18] Dai J, Xu C X and Sun X W 2011 *Adv. Mater.* **23** 4115
[19] Aguilar C A, Haight R, Mavrokefalos A, Korgel B A and Chen S C 2009 *ACS Nano* **3** 3057
[20] Lin D, Wu H, Zhang W, Li H and Pan W 2009 *Appl. Phys. Lett.* **94** 172103
[21] Xu C, Dai J, Zhu G, Zhu G, Lin Y, Li J and Shi Z 2014 *Laser Photon. Rev.* **8** 469
[22] Czekalla C, Sturm C, Schmidt-Grund R, Cao B, Lorenz M and Grundmann M 2008 *Appl. Phys. Lett.* **92** 241102
[23] Lu J, Zhu Q, Zhu Z, Liu Y, Wei M, Shi Z and Xu C 2016 *J. Mater. Chem. C* **4** 7718
[24] Lu J, Li J, Xu C, Li Y, Dai J, Wang Y and Wang S 2014 *ACS Appl. Mater. Interfaces* **6** 18301